Iowa State University
Digital Repository

Geological and Atmospheric Sciences Publications | Geological and Atmospheric Sciences

10-2000

Sensitivity of forecast rainfall in a Texas convective system to soil moisture and convective parameterization

William A. Gallus Jr.
Iowa State University, wgallus@iastate.edu

Moti Segal
Iowa State University, segal@iastate.edu

Follow this and additional works at: http://lib.dr.iastate.edu/ge_at_pubs

Part of the Agronomy and Crop Sciences Commons, Atmospheric Sciences Commons, and the Geology Commons

The complete bibliographic information for this item can be found at http://lib.dr.iastate.edu/ge_at_pubs/26. For information on how to cite this item, please visit http://lib.dr.iastate.edu/howtocite.html.

This Article is brought to you for free and open access by the Geological and Atmospheric Sciences at Iowa State University Digital Repository. It has been accepted for inclusion in Geological and Atmospheric Sciences Publications by an authorized administrator of Iowa State University Digital Repository. For more information, please contact digirep@iastate.edu.

Sensitivity of forecast rainfall in a Texas convective system to soil moisture and convective parameterization

Abstract

The impact of soil moisture on the forecast of a small-scale convective system, and sensitivity of results to the convective parameterization used, are investigated through Eta Model simulations (run in an operational-like setting) of a convective system occurring on 27 May 1997 in Texas. The event was influenced by a southwestward-propagating gravity wave from early morning convection in Arkansas that intersected a slow-moving cold front, releasing extreme conditional static instability. Isolated heavy rainfall, over 100 mm, occurred in some regions. A control simulation with 22-km horizontal resolution reasonably simulated the event, even though mesoscale influences such as the gravity wave important to this event are often poorly captured by numerical models. A series of sensitivity tests were performed to examine the impact of soil moisture on the simulations. Two different convective parameterizations were used for the tests. Although domain average precipitation is found to generally vary in a straightforward way with soil moisture, peak precipitation in the regions of intense convection shows more complex behavior. Sensitivity of precipitation amounts to soil moisture differs significantly among runs having different convective parameterizations. For instance, with the Kain-Fritsch convective scheme, relatively dry soil is found to result in stronger convective outflows that converge with stronger ambient flow to greatly enhance the precipitation in the region where heaviest rainfall occurs. With the Betts-Miller-Janjic scheme, drier soil generally results in less precipitation than in the control run, although some enhancement in peak amount does occur within a narrow range of drying. The differences between the peak quantitative precipitation forecasts in the runs is primarily due to the inclusion of a convective downdraft in the Kain-Fritsch parameterization, and its impact on secondary convective development. Additional sensitivity tests find limited impact from prescribed vegetation coverage. A final sensitivity test shows that precipitation amounts are even more strongly affected by the vertical resolution of the data used to initialize the shallow but moist boundary layer than by variations in the soil moisture or vegetation fraction.

Keywords

Agronomy, atmospheric temperature, atmospheric turbulence, computer simulation, gravity waves, moisture, soils, vegetation, wave propagation, weather forecasting, convective system, forecast rainfall, soil moisture, rain, convective system, numerical model, sensitivity analysis, soil moisture, weather forecasting, United States

Disciplines

Agronomy and Crop Sciences | Atmospheric Sciences | Geology

Comments

This article is from *Weather and Forecasting* 15 (2000): 509, doi: 10.1175/1520-0434(2000)015<0509:SOFRIA>2.0.CO;2. Posted with permission.

This article is available at Iowa State University Digital Repository: http://lib.dr.iastate.edu/ge_at_pubs/26

Sensitivity of Forecast Rainfall in a Texas Convective System to Soil Moisture and Convective Parameterization

WILLIAM A. GALLUS JR.

Department of Geological and Atmospheric Science, Iowa State University, Ames, Iowa

MOTI SEGAL

Department of Agronomy, Iowa State University, Ames, Iowa

(Manuscript received 24 August 1999, in final form 6 June 2000)

ABSTRACT

The impact of soil moisture on the forecast of a small-scale convective system, and sensitivity of results to the convective parameterization used, are investigated through Eta Model simulations (run in an operational-like setting) of a convective system occurring on 27 May 1997 in Texas. The event was influenced by a southwestward-propagating gravity wave from early morning convection in Arkansas that intersected a slow-moving cold front, releasing extreme conditional static instability. Isolated heavy rainfall, over 100 mm, occurred in some regions.

A control simulation with 22-km horizontal resolution reasonably simulated the event, even though mesoscale influences such as the gravity wave important to this event are often poorly captured by numerical models. A series of sensitivity tests were performed to examine the impact of soil moisture on the simulations. Two different convective parameterizations were used for the tests. Although domain average precipitation is found to generally vary in a straightforward way with soil moisture, peak precipitation in the regions of intense convection shows more complex behavior. Sensitivity of precipitation amounts to soil moisture differs significantly among runs having different convective parameterizations. For instance, with the Kain–Fritsch convective scheme, relatively dry soil is found to result in stronger convective outflows that converge with stronger ambient flow to greatly enhance the precipitation in the region where heaviest rainfall occurs. With the Betts–Miller–Janjic scheme, drier soil generally results in less precipitation than in the control run, although some enhancement in peak amount does occur within a narrow range of drying. The differences between the peak quantitative precipitation forecasts in the runs is primarily due to the inclusion of a convective downdraft in the Kain–Fritsch parameterization, and its impact on secondary convective development.

Additional sensitivity tests find limited impact from prescribed vegetation coverage. A final sensitivity test shows that precipitation amounts are even more strongly affected by the vertical resolution of the data used to initialize the shallow but moist boundary layer than by variations in the soil moisture or vegetation fraction.

1. Introduction

On 27 May 1997, a significant tornado outbreak with substantial loss of life occurred in parts of central Texas, with F5 damage attributed to one tornado. Large-scale weather features on the morning of 27 May did not look especially favorable for significant tornadoes (Corfidi 1998), with relatively weak winds aloft (30 kt or less at 500 mb, 35 kt at 300 mb). As is often the case when large-scale forcing is relatively weak, mesoscale boundaries strongly influenced the development of the event. A weak cold front moving slowly to the southeast played some role in the development of convection, along with a prefrontal trough and an internal gravity wave (Corfidi 1998). In addition, extreme conditional static instability apparently compensated for more modest vertical wind shear to assist the development of intense tornadoes (e.g., Rasmussen and Wilhelmson 1983). The tornadic thunderstorms organized into a small-scale convective system that produced isolated heavy rainfalls.

The operational Eta Model (with 48-km horizontal resolution) forecasted small amounts of precipitation ($<$20 mm) in the south-central part of Texas. However, higher horizontal resolution versions of the model [comparable to resolutions proposed for use operationally in 2000 (S. Weiss, SPC, 2000, personal communication)] appeared capable of simulating many of the key components of the convection that occurred on this day (i.e., southwestward propagation, timing of significant rainfall, maximum rainfall in far southern Texas). These

Corresponding author address: Dr. William A. Gallus Jr., Dept. of Geological and Atmospheric Science, Iowa State University, 3025 Agronomy Hall, Ames, IA 50011.
E-mail: wgallus@iastate.edu

© 2000 American Meteorological Society

simulations produced much heavier precipitation than in the operational run. As the high moisture content in the lower atmosphere appeared to be conducive to the development of intense convection, it is intriguing to explore in detail the sensitivity of the related rainfall fields to the moisture availability—in particular, the corresponding sensitivity to variations in soil moisture, and the initial atmospheric moisture field.

Modification of soil moisture has the following impacts on cold fronts accompanied by convection: (i) increased soil moisture and thus evapotranspiration enhances thermodynamically the potential for convection, (ii) cloud cover persisting in the cold sector behind the front intensifies the cross-front temperature gradient as the soil in the warm frontal sector becomes drier (Segal et al. 1993) (in the present case study, it appears that this effect was not active as no significant cross-front cloud contrast existed before the initiation of convective activity), and (iii) increased soil moisture results in a less developed convective boundary layer (CBL) and reduced cross-isobaric flow. Studies of the related impact on convergence at the frontal surface in idealized 2D cases (e.g., Becker et al. 1997) have not found consistent effects on frontal precipitation patterns. It appears that case studies matching real atmospheric situations would be useful to provide further insight into the sensitivity of cold front associated convection to surface diabatic forcing.

Past studies of convective events have found that surface moisture can influence the evolution of the convection and precipitation. Lanicci et al. (1987) showed that variable soil moisture conditions in the southern plains were important for generating differential surface heating and low-level instability through strong surface evaporation. The soil moisture variations played a role in where the lid, or elevated mixed layer, would be removed and, thus, where and when convection would occur. Koch et al. (1997) found that reduced soil moisture in a simulation resulted in a stronger squall line ahead of a cold front than in a simulation with wetter soil. The drier soil apparently improved the low-level convergence near the front. Gallus and Segal (1999) similarly noted a tendency toward enhancement of frontal convergence with a decrease in soil moisture for a late winter cold front case. In some environments, the enhanced convergence may more than compensate for generally less favorable lower-tropospheric thermodynamics associated with drier soil (e.g., Segal et al. 1995; Clark and Arritt 1995). Evaluating soil moisture impacts on summer rainfall in the central United States using the Pennsylvania State University–National Center for Atmospheric Research fifth-generation Mesoscale Model, Pan et al. (1996) noted a sensitivity to the selected cumulus parameterization.

In order to establish the general response of precipitation to surface moisture under common warm season conditions of a weak front and large conditional static instability, there is a need to examine a variety of real-world situations. To support operational forecasting, it would be advantageous to adopt a similar model setting to that used by the National Centers for Environmental Prediction (NCEP). The 27 May 1997 Texas intense convective event provides a good case for such evaluation. It is the purpose of this paper to examine some potential impacts of soil moisture through sensitivity tests performed for this case. Two different convective schemes are used to investigate the uniformity of the soil moisture–precipitation impact. In addition, sensitivity to vegetation coverage and the vertical resolution of the data used to initialize the moist boundary layer are also examined to help put the soil moisture impacts into perspective. The event was not well forecast by operational numerical models and forecasters early in the day and seemed dependent upon subtle, mesoscale features. Because large-scale forcing was generally weak, it is believed that this event serves as a good case for an investigation into potential impacts from surface processes.

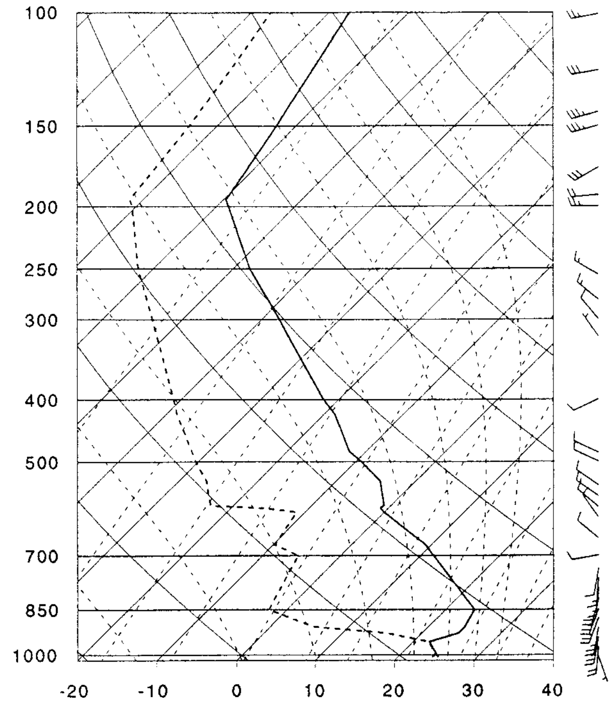

FIG. 1. Skew T–log$p$ diagram from Corpus Christi, TX, at 1200 UTC 27 May 1997. Temperature (solid) and dewpoint (dashed) are plotted.

2. Observational background

On the morning of 27 May, a southwest–northeast-oriented cold front was moving slowly across Texas. Very humid conditions were present in a shallow layer (~100 mb deep) near the ground ahead of the front. Although no soundings were available from the region of central Texas that would later experience the most intense convection, a thermodynamic profile (Fig. 1)

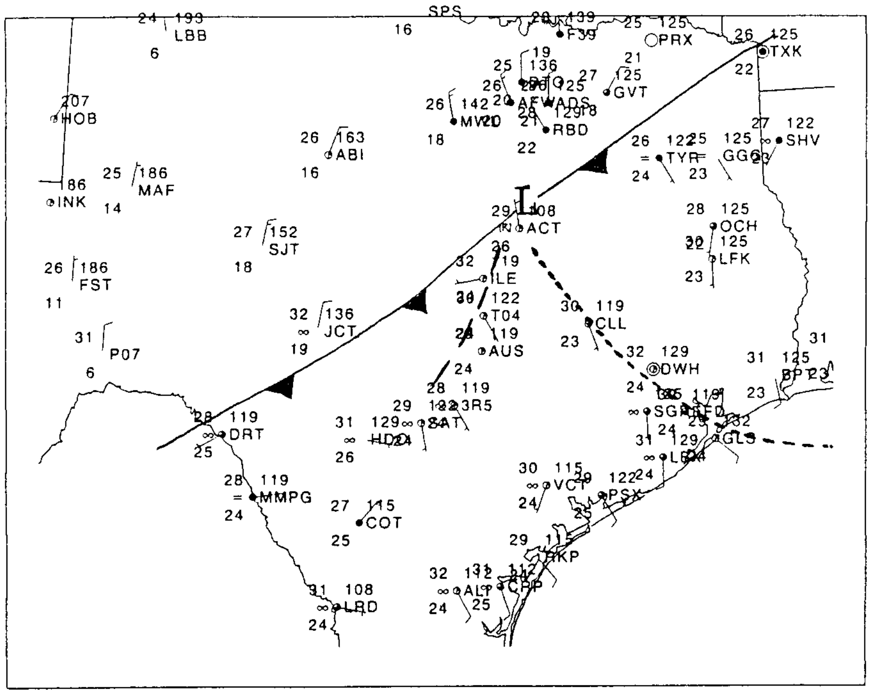

FIG. 2. Surface map at 1800 UTC 27 May (from Gallus 1999). Conventional notation is used for fronts. Location of gravity wave (inferred from satellite data) indicated with short-dashed line. Station plot includes temperature (upper left) and dewpoint (lower left) in °C, altimeter setting (tenths of mb, leading 10 dropped), and winds (m s^{-1}; full barb is 5 m s^{-1}).

from Corpus Cristi (CRP) on the Gulf coast (see Fig. 2 for location), south of the region of later convective development, shows a shallow but significant moist boundary layer, capped by a lid of somewhat warmer and drier air above ~950 mb. Soundings from other sites around the region were generally similar. This lower-tropospheric vertical structure is common in the southern plains during the spring and summer, and presents a forecasting challenge (Bluestein 1993). The elevated inversion can allow the boundary layer to become very warm and humid, but can prevent the release of substantial conditional static instability. Under these conditions, soil moisture can play a significant role in determining which, if any, air parcels can rise to their level of free convection and, thus, also on the location and timing of any convective precipitation that develops.

Dewpoint temperatures at 850 mb at all rawinsonde sites in or near Texas east of the front were dry (~0°C), with the exception of Del Rio (DRT), which had a dewpoint of 7°C. The higher dewpoint at 850 mb in DRT may be due in part to the slightly higher elevation of the station (307 m). However, it is also likely that the DRT sounding is depicting the somewhat deeper boundary layer present just ahead of the cold front, where evapotranspiration and low-level convergence have moistened and deepened the CBL in a region of ascent.

By 1800 UTC (Fig. 2), the cold front had moved less than 50 km since 1200 UTC, and extended from around DRT northeastward to Texarkana (TXK). Significant moisture convergence had been occurring along a trough in this region all morning, and surface dewpoints had risen by ~2°C (corresponding to an increase of ~2.2 g kg^{-1} in the specific humidity) since 1200 UTC to between 24° and 26°C due most likely to the effects of evapotranspiration. Considering a well-mixed CBL of 1000-m depth, the increase of specific humidity for the first half of the day corresponds to evapotranspiration of 2.2 mm, or 4.4 mm for the entire day, implying moderately wet soil. A west wind at Killeen (ILE) may have been evidence of a boundary ahead of the front. Using a series of satellite images, Corfidi (1998) documented a gravity wave that was propagating southwestward and approaching Waco (ACT) at this time (shown with dotted line in Fig. 2; position obtained from satellite imagery). The gravity wave appeared to enhance developing convection near Waco.

A modified sounding near Austin (AUS) at 1800 UTC, based on Geostationary Operational Environmental Satellite (GOES) sounder estimates (D. Gray, NESDIS, 1998, personal communication) and 0000 UTC information from DRT, showed extremely large conditional static instability (Fig. 3; from Gallus 1999). The moist layer had deepened compared to 1200 UTC soundings, due to the sustained moisture convergence. GOES sounder–derived estimates of precipitable water showed a narrow axis of enhanced values near the front, with up to 52 mm in this region, compared with ~45

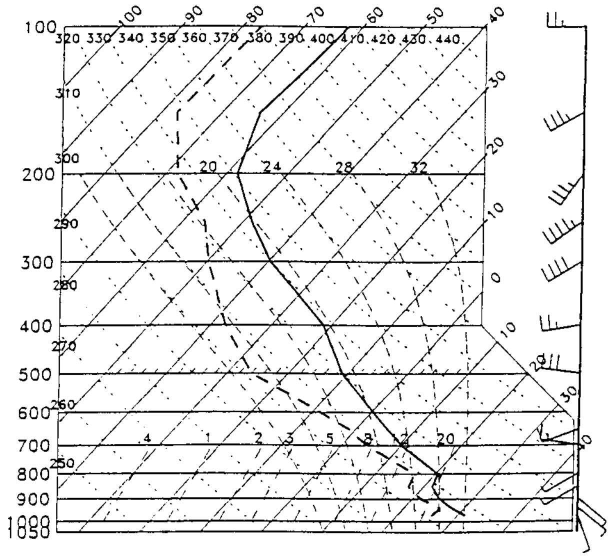

FIG. 3. Skew *T*–log*p* diagram (estimated) from Austin in central Texas at 1800 UTC 27 May 1997 (from Gallus 1999). Temperature (solid) and dewpoint (dashed) are plotted.

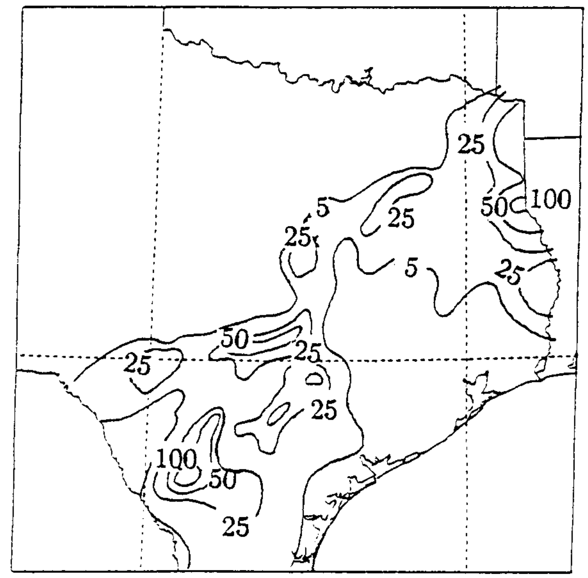

FIG. 4. Observed precipitation (mm) determined from National Oceanic and Atmospheric Administration *Climatological Data* publication for the period 1200 UTC 27 May to 0600 UTC 28 May 1997 (from Gallus 1999). Contours are 5, 25, 50, and 100 mm.

mm farther east in Texas. The precipitable water in the ~1000 m layer near the surface was 18–21 mm. Surface-based convective available potential energy (CAPE) values exceeded 5500 J kg^{-1} over most of central and eastern Texas at this time (Corfidi 1998).

Over the next several hours, tornadic thunderstorms propagated in a motion strongly deviant to the mean flow, generally along the prefrontal trough, toward the south-southwest. Darkow and McCann (1977) have also identified other extreme right-moving supercells associated with high instability and weak shear. Numerous tornados occurred in this event including several rated F3 or higher on the Fujita scale. The most intense of these hit the town of Jarrell (between sites T04 and ILE in Fig. 2) just after 2030 UTC. Strong winds and flash flooding due to 50–125 mm of rainfall occurred in scattered areas from near Austin southwest toward Cotulla (COT) near the Mexican border (Fig. 4; from Gallus 1999). The convection developed more of a southeastward propagation after 0000 UTC, with rainfall spreading toward the Gulf coast.

3. Model configuration

For all simulations, the Eta Model (a version comparable to the operational version used in late 1998) was run with a ~2000 km × 2000 km domain centered on the southern plains of the United States. [A detailed description of the Eta Model can be found in Mesinger et al. (1988) and Janjic (1994).] Vertical resolution generally varied from around 125 m in the lowest of 32 model layers to around 1 km at model top. Initial and boundary condition data were supplied from a University Corporation for Atmospheric Research Unidata feed of 80-km Eta datasets generated from the then-48-km operational run. Simulations were initialized at 1200 UTC 27 May so that at least 6 h passed before the primary convective event developed.

Soil moisture and temperature data were supplied from the NCEP 40-km horizontal resolution Global Energy and Water Cycle Experiment (GEWEX) Continental Scale International Project (GCIP) archive and adjusted from the original two layers to the seven layers used in the high-resolution version of the model. Gridded fields of eight soil types and 12 vegetation types were determined from Environmental Protection Agency and United Nations Food and Agriculture Organization datasets, respectively. Topography data were provided from a 30″ United States Geological Survey dataset. Vegetation coverage in the model was prescribed based on vegetation type and was characteristically 0.5 throughout the central Texas region (where the primary convective event occurred). As will be discussed later, the sensitivity of results to the prescribed vegetation coverage was small.

A control simulation was run using 22-km horizontal resolution (compared with 48-km resolution used operationally at the time), the Betts–Miller–Janjic (BMJ) convective scheme used operationally, and soil moisture data unadjusted from the NCEP GCIP archive. Although the 22-km resolution is insufficient to resolve individual thunderstorms, and higher resolution could better simulate the interaction of mesoscale boundaries, this resolution was chosen because it represents that proposed for operational use in 2000. The choice of model resolution and soil initialization dataset to match the operational setting should assist in application of the re-

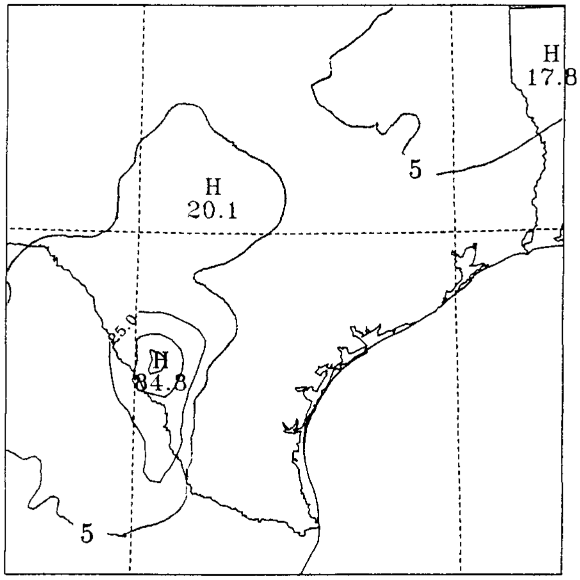

FIG. 5. Simulated precipitation (mm) for the period 1200 UTC 27 May to 0600 UTC 28 May 1997 with the BMJ scheme at 22-km horizontal resolution. First contour is 5 mm; otherwise contour interval is 25 mm.

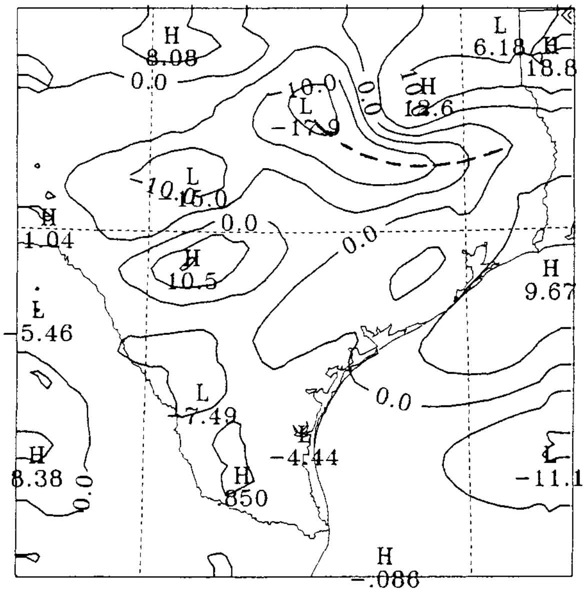

FIG. 6. Simulated surface moisture divergence ($\times 10^{-4}$ g kg^{-1} s^{-1}) at 1500 UTC 27 May 1997 from a 22-km horizontal resolution run. Contour interval is 5×10^{-4} g kg^{-1} s^{-1}. Apparent mesoscale boundary indicated with a dashed line.

search to improve operational forecasting. Additionally, sensitivity tests were performed using 22-km horizontal resolution with a wide range of variations in initialized volumetric soil moisture (covering highly dry to highly wet soil conditions). To put the soil moisture impacts into perspective, additional sensitivity tests were run to determine the impact of changes in vegetation coverage (termed vegetation fraction in the Eta Model) and the impact of a more poorly resolved moist boundary layer in the initialization (initial data with 50-mb vertical resolution were replaced with data at 1000 and 850 mb only in the lower troposphere).

The version of the Eta Model used includes a modified Oregon State University (OSU) parameterization (e.g., Pan and Mahrt 1987; Holtslag and Ek 1996; Chen et al. 1996) essentially similar to the Noilhan and Planton (1989) scheme capturing the main biophysical controls on evapotranspiration. It was felt that the land surface parameterization of the model could reasonably simulate the important processes for this case. Multiple 1D, 2D, and 3D sensitivity experiments with the model suggested no serious weaknesses in the model's ability to simulate surface exchange processes. However, Yucel et al. (1998) have identified a few biases in the scheme that could adversely affect results, especially for simulations longer than those used in this study.

The moist physics in the model include the modified BMJ convective parameterization (Betts 1986; Betts and Miller 1986; Janjic 1994) with both shallow and deep convection, and an explicit cloud water parameterization (Zhao et al. 1991). Vertical turbulent exchange is calculated based on the Mellor–Yamada level-2.5 model (Mellor and Yamada 1974, 1982) with some recent modifications (Lobocki 1993; Gerrity et al. 1994). A seven-layer version of the modified OSU soil model with a vegetation canopy is used for land surface physics. Soil moisture and temperature are explicitly forecast along with a surface skin temperature. Seven soil layers were adopted to provide adequate resolution needed for the prediction of these variables. Evapotranspiration comprises three components, including direct evaporation from the soil surface, direct evaporation from wet vegetation (of intercepted rain or dew), and transpiration from the vegetation canopy. For some sensitivity tests, the Kain–Fritsch (KF) convective parameterization was substituted (Kain and Fritsch 1993). A discussion of the basic differences between the two schemes is found in Gallus (1999).

4. Control simulation

The model with the BMJ scheme simulated well the timing and general area of rainfall in the May 27 case (Fig. 5; this figure and others show a pertinent subset of the model's full simulation domain). The maximum precipitation occurred within a small region near the Texas–Mexico border, within about 50 km of the observed maximum. In the model, an area of convective precipitation during the first 2 h of integration (1200–1400 UTC) in far eastern Texas generated a boundary that propagated west-southwestward. The boundary can be seen as a northwest–southeast arc-shaped region of enhanced simulated moisture convergence at 1500 UTC in Fig. 6. The region of rainfall has resulted in significant moisture divergence in northeastern Texas into northern

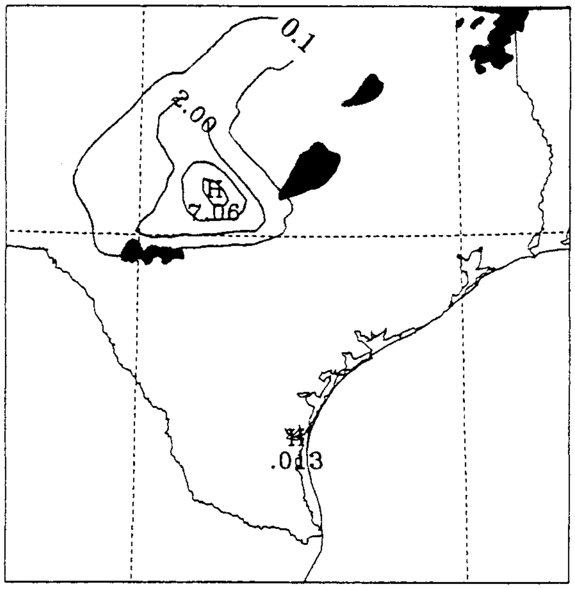

FIG. 7. Simulated hourly precipitation during 2000–2100 UTC 27 May using the BMJ scheme at 22-km horizontal resolution (contours at 0.1, 2, 4, and 6 mm) with observed precipitation regions overlaid [from the NCEP stage IV 4-km radar-based analysis; M. Baldwin, NCEP (2000, personal communication)].

Louisiana. The front can be seen as a southwest-northeast band of enhanced moisture convergence. The convective boundary initially moved westward with a speed of around 18 m s^{-1}. It slowed gradually after 1500 UTC as it approached the persistent area of moisture convergence along the front in central Texas.

The boundary in the model did not appear to be a gravity wave. Strongest cross-boundary flow perturbations were in the region of strongest pressure gradient, as would be expected with an outflow boundary. The BMJ convective parameterization does not allow for parameterized convective downdrafts. However, grid-scale precipitation can result in evaporative cooling and a modest cold pool. In this case, however, the temperature decrease at the surface behind the boundary was small (not shown). Larger temperature decreases occurred above the surface and thus the boundary seems to be an artifact of the parameterization's adjustment of temperature toward a reference profile, something of a ''pseudo''-outflow boundary. Although activation of the BMJ scheme generally warms most model layers, in some cases cooling can occur at relatively low levels within the cloud (M. Baldwin, SPC, 1999, personal communication). It is thus possible that a fairly accurate simulation of the event was obtained with incorrectly depicted forcing. However, both the model's boundary and the observed gravity wave resulted in ascent important for initiating significant convection, and it is unlikely the differences in the triggering mechanism adversely affect the model results of sensitivity to soil moisture shown later.

The strong moisture convergence presented in Fig. 6 resulted in large conditional static instability (nearly adiabatic lapse rates with high surface moisture) in the model at 1800 UTC, similar to that estimated from satellite sounders. Although some small amounts of precipitation were simulated along the westward-propagating boundary throughout the morning, heavier precipitation began developing in the model around 1900 UTC, roughly 60 km west of Waco. The timing was within 1–2 h of the observed first intense storm, although the location was displaced westward (the observed storm was much closer to Waco). A comparison of the model precipitation in the hour ending at 2100 UTC, and radar-estimated precipitation (from the NCEP stage IV 4-km analysis) for the same time (Fig. 7), shows a westward displacement (and a failure to show additional small-scale convection in other areas along the front). It should be noted that the model's 22-km horizontal resolution is much coarser than the 4-km resolution of the analysis; two of the four general clusters of rainfall occur over areas no larger than one or two model grid boxes. The westward displacement of the simulated precipitation in this portion of Texas (relative to the largest region of observed significant rainfall) is associated with the westward movement of the simulated cold front relative to observations. The westward shift in precipitation also occurred in the operational Eta and may suggest an overestimate of the strength of the larger-scale upper-level trough exiting the Rocky Mountains (inducing surface pressure falls in the lee of the mountains). The core of heaviest model precipitation tracked south-southwest during the afternoon, again agreeing with observations (not shown). By 0600 UTC, the model showed two areas of enhanced rainfall (Fig. 5), one near AUS with 20 mm, and a more significant one (85 mm) to the south. The simulated precipitation near Austin fell just prior to 0000 UTC (1900 LDT), while the heavier precipitation to the south occurred in the evening (after 0000 UTC).

It should be noted at this point that the Gallus (1999) simulations of this event, using a domain slightly farther to the north, had somewhat larger precipitation amounts in far southern Texas, where the peak precipitation with 22-km resolution was around 100 mm. In those simulations, this precipitation maximum was close to the edge of the model domain. The difference in results occurring as the lateral boundaries are moved farther from the region of mesoscale forcing reiterates the concerns of Warner et al. (1997) regarding negative impacts of limited domains on mesoscale simulations. For this event, significant differences were confined to the southern precipitation maximum, which was only a few grid points from the lateral boundary in Gallus (1999). The current domain configuration reduces any problems from lateral boundaries.

5. Model sensitivity simulations

a. Sensitivity to resolution and convective scheme

Gallus (1999) found that maximum storm precipitation in the Eta Model for this event when the BMJ

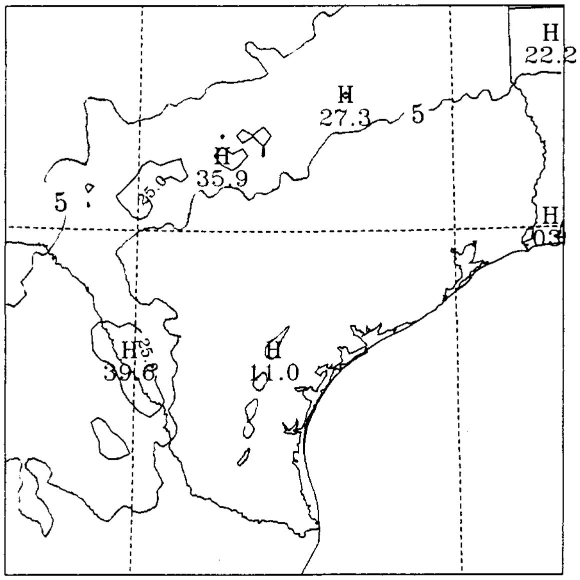

FIG. 8. As in Fig. 5 except for the Eta simulations with the KF convective parameterization.

scheme was used was extremely sensitive to the horizontal grid resolution. The general shape of the rainfall region was relatively unchanged as resolution varied from 78 to 12 km, but finer details of the field were resolved at higher resolutions. The BMJ scheme contributed most of the precipitation at coarse resolutions, but its contribution fell to less than 20% of the total precipitation at 12-km resolution. That study also found that the horizontal resolution dependence of precipitation was significantly different when the BMJ scheme was substituted with the KF scheme.

When the KF scheme was used, the scheme activated early, in association with strong moisture convergence along the front. The KF scheme uses a trigger function based on grid-resolved vertical motion. The strong vertical motion along the front was sufficient to remove any convective inhibition. By 1800 UTC, precipitation was produced in the model all along the front (see Fig. 22 of Gallus 1999). Unlike the BMJ run, a westward-propagating convective boundary was not obvious in the KF results; the first significant rainfall was not restricted to a small area near Waco. Steady production of precipitation continued through the end of the simulation at 0600 UTC 28 May. The precipitation pattern with the KF scheme was somewhat more uniform than with the BMJ scheme, and regions of intense precipitation were not as distinct as those simulated with the BMJ scheme (Fig. 8). The convective component of the precipitation dominated, and the horizontal resolution dependence of the peak precipitation was much less than in the BMJ runs.

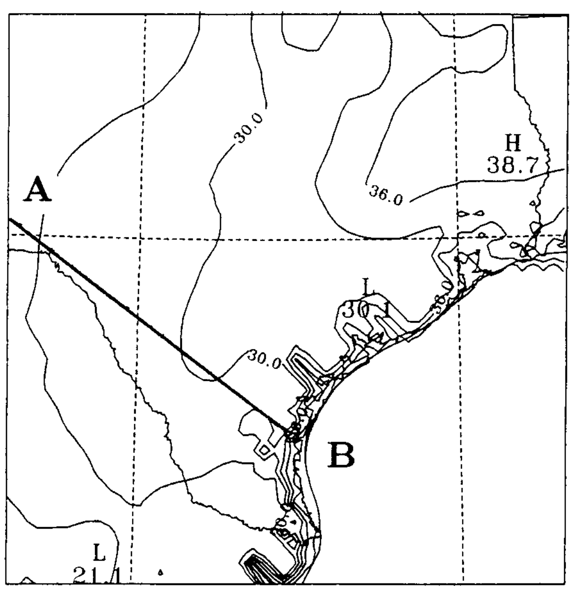

FIG. 9. Initial volumetric soil moisture (in %) in the upper soil layer for the control case. Contour interval is 3%. Line A–B indicates location of vertical cross sections shown in Figs. 12, 13, and 16.

b. Sensitivity to soil moisture

1) INITIAL SOIL MOISTURE

As stated previously, the change in the surface Bowen ratio (ratio of sensible to latent surface heat flux) affects the CBL thermodynamic characteristics and corresponding convective features. Also, in locations affected by cold fronts, the frontal convergence may intensify/weaken in response to changes in the Bowen ratio. To evaluate such impacts on the simulated precipitation field, a series of sensitivity tests were performed in which the initialized volumetric soil moisture was increased or decreased in 10% increments from its control value, spanning the range from 60% drier than control to 30% wetter. (The volumetric soil moisture is the ratio of the water volume to the soil volume being considered; the saturation volumetric moisture occurs when the entire volume of the soil pores is occupied by water, and it is the maximum volumetric soil moisture possible.) The selected soil volumetric moisture range provides a reasonable sample from very low to very high for Bowen ratio values.

The control simulation initial volumetric soil moisture field is depicted in Fig. 9. In general, horizontal soil moisture gradients were modest across Texas, unlike some other events (e.g., Koch et al. 1997). Chang and Wetzel (1991) have demonstrated an important influence of soil moisture gradients on one small-scale tornadic convective system. Additionally, Ookouchi et al. (1984) suggested that sharp horizontal soil moisture gradients may generate thermal circulations as strong as sea breezes and, thus, may trigger convection. However, no *observational* support has been documented for such strong circulations. Overall, it is unlikely that spatial

TABLE 1. Soil volumetric wetness (θ; in %) physical characteristics. The values of θ_{pwp}, θ_{ref}, and θ_w are based on the Eta calibrations. The values of θ_{fc} are based on Clapp and Hornberger (1978). See text for notation definition.

Soil type	θ_{pwp}	θ_{ref}	θ_w	θ_{fc}
Silty clay loam	11.9	38.7	14.0	32.2
Clay loam	10.3	38.2	16.0	32.5

variations in the soil moisture were of sufficient magnitude to play a role in the dynamical (i.e., through thermal-induced circulations) forcing of convection on this day. Volumetric soil moisture was generally near 30% in central Texas, with slightly higher values to the east and lower values to the west. These values seem reasonable considering that several precipitation systems had dropped 25 mm or more of rain per event in much of central and eastern Texas in the previous 2–3 weeks, with a 1–2-week dry spell ongoing farther west, where substantial rainfall had occurred in early May. The rainfall event that occurred throughout central Texas a few days prior to the 27 May event was surprisingly uniform and widespread, with cooperative observer reports (~20–40 km resolution) from the publication *Climatological Data* showing at least 25 mm over the entire region. Thus, no available data suggest any patchiness or tight gradients in the soil moisture for this event. For the soil types in this region, medium or medium–fine (Zobler 1986), silty clay loam, or clay loam (Cosby et al. 1984), the saturation volumetric moisture is around 46%, with the wilting point for vegetation being 10%–12%. Thus, the variations used in the initial soil moisture field nearly span the range of values between these significant levels.

To add insight into the physical meaning of the sensitivity simulations, we provide values of pertinent volumetric soil moisture (θ) for appropriate soil textures in Table 1. In the Eta soil module, the transpiration response to changes in soil moisture is related to θ_{pwp} and θ_{ref}, the plant wilting point and reference volumetric soil moisture, respectively. When $\theta \leq \theta_{pwp}$, transpiration is zero, and when $\theta > \theta_{ref}$, the transpiration is the same as at θ_{ref}. For $\theta_{pwp} \leq \theta \leq \theta_{ref}$, the change in transpiration is linear. When bare soil is considered, similar variations occur, but with θ_w and θ_{fc}, the wilting point and the field capacity, respectively, as the corresponding approximate lower and upper limits for the evaporation response function.

2) Soil moisture impact on domain-average precipitation

The sensitivity simulations were done with both the BMJ and KF convective parameterizations. Total domain-integrated precipitation after both 12 and 18 h can be seen in Fig. 10. During the first 12 h of integration, simulations with both convective schemes showed a rather smooth increase in total domain precipitation as

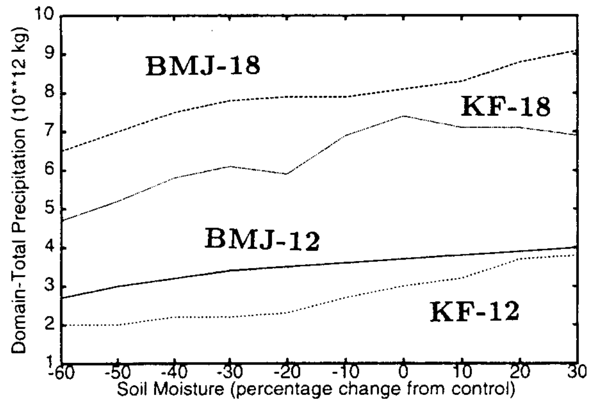

FIG. 10. Total domain-integrated precipitation (in 10^{12} kg) for 12 h ending at 0000 UTC and 18 h ending at 0600 UTC for a series of simulations with differing initial soil moisture contents using the BMJ and KF convective parameterizations.

soil moisture content was increased. This is the time period when tornadic storms were first observed in central Texas. In the sensitivity tests, precipitation amounts of 10–35 mm were common in the region near Austin.

During the next 6 h (evening and early night local time), the heaviest simulated precipitation occurred in southern Texas, roughly agreeing with observations. Total domain precipitation began to show more variability with changes in soil moisture during this time of intense convection. For runs with the BMJ parameterization, total domain precipitation continued to increase rather smoothly for increasing soil moisture, particularly for values moister than the control. Relatively little sensitivity was present for small reductions in soil moisture, but a more rapid decrease in domain precipitation occurred for soils 40% or more drier than the control value.

For runs with the KF scheme, the behavior of total domain precipitation was more complicated. The largest values of total domain precipitation occurred in the control run, with a secondary weak maximum for a 30% reduction in soil moisture from the control value. Wetter soils decreased the total domain precipitation uniformly from the large value occurring in the control run, but in general, the values were larger than those found for drier soils.

3) Soil moisture impact on peak gridpoint precipitation

To better understand the variations in total domain precipitation, it is important to examine the smaller-scale details of the precipitation fields in all simulations. Peak storm precipitation (i.e., maximum amount at any grid point) accumulated during 12- and 18-h periods can be seen in Fig. 11. It should be noted that the peak precipitation may be associated with different convective areas in the sensitivity tests. In simulations with the BMJ scheme (Fig. 11a), little difference can be seen in the peak amounts at 12 h into the integration. Nearly

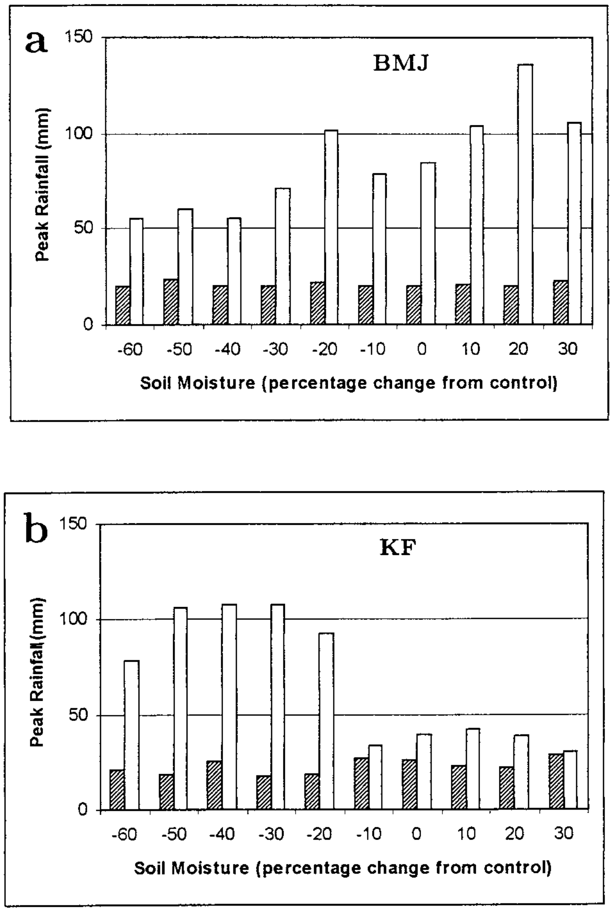

FIG. 11. Peak 12-h (shaded bars) and 18-h (clear bars) precipitation (mm) within the domain for a series of simulations with differing initial soil moisture contents using the (a) BMJ and (b) KF convective parameterizations.

all of the peak precipitation (>98%) is produced by the BMJ convective scheme (not shown).

Noticeably larger differences in peak rainfall occur by 18 h, however, when local maxima are present for soils both 20% wetter and 20% drier than the control volumetric soil moisture. In general, wetter soils increase the peak precipitation over the control value, with the maximum increase exceeding 50% for the 20% wetter soil. Further wetting of the soil, however, reduces the peak precipitation from this maximum value. Drier soils generally result in less peak precipitation, with the exception of a local maximum for a 20% reduction in soil moisture. The convective contribution is relatively uniform throughout the sensitivity tests, around 40 mm, with little dependence on the soil moisture. Thus, the convective contribution is relatively greater at the driest soils (where the total precipitation amounts are smallest). In the BMJ runs, the peak rainfall generally remains in south Texas near Cotulla in all of the runs.

In simulations with the KF scheme (Fig. 11b), the pattern is different, as should be expected since the scheme activates much faster than the BMJ scheme, and the precipitation field is substantially different. During the first 12 h of the simulation, the peak rainfalls are somewhat variable with respect to soil moisture. The heaviest amount occurs with the wettest soil, but other maxima occur with the control soil moisture value and with 40% drier than control soil moisture. All of the precipitation in the first 12 h in all sensitivity tests is produced by the KF convective scheme.

At 18 h, the KF simulations show a marked tendency for greater peak precipitation to occur with drier soil. A 10% decrease in soil moisture from the control value results in a small decrease in peak precipitation, but for even drier soils, the peak rainfall amounts nearly triple from the control value. The maximum amount, 108 mm, occurs for both the 30% and 40% reduction in the volumetric soil moisture from control. Peak rainfall does not begin to diminish appreciably until soil moisture is 60% drier than control. The large increase in predicted rainfall (more than doubling) that occurs as volumetric soil moisture decreases by only 10% (from 10% drier than control to 20% drier) suggests that even small errors in simulated soil moisture may significantly affect a forecast under some circumstances.

Although it would be beneficial in interpreting model precipitation guidance for forecasters to evaluate how well the model's initialized soil moisture field agrees with observations, measurements of surface moisture are not readily available, complicating this evaluation. In addition, a substantial sensitivity of precipitation to soil moisture implies that an incorrect production of precipitation early in a model simulation could seriously impact the simulation of later events, if the earlier simulated event changes the soil moisture. The heaviest amounts in these drier soil simulations occur in a region where convection develops late (after 0000 UTC) and is influenced by the earlier convection to the north. Unlike the BMJ runs, the location of peak precipitation in the KF runs varies greatly between the wetter soil runs and the drier soil runs. In the wet soil runs, precipitation in south Texas is substantially reduced, so that the peak amounts are in the west-southwest–east-northeast band across central Texas.

The behavior of the peak precipitation for wetter soil is the reverse of the dry cases. A small increase in soil moisture enhances peak rainfall by a small amount, but further increases significantly decrease the peak precipitation.

The convective component is slightly more variable in the KF runs than in the BMJ runs, but it is not responsible for the large trends in the total peak precipitation. For the wettest soils, the KF convective component is 90%–100% of the total precipitation. In the control run, around 85% of the total precipitation is generated by the scheme. The large increases that occur with dry soil are entirely due to enhancement of grid-resolved precipitation, with the convective component generally falling to under 30% of the total.

4) Soil moisture impact on low-level thermodynamics and winds

Some insight into the reasons for the significant increase in peak precipitation as soil moisture is reduced can be gained by examining the low-level thermodynamic and wind fields during the event. A comparison of the evolution of events in the control and 40% drier than control soil moisture cases (both with the KF scheme) shows significant changes in both the low-level thermodynamics and winds. [Although the following comparison concentrates on the 40% drier soil sensitivity test because of the large difference between its peak quantitative precipitation forecast (QPF) and the control run, the changes in the fields from the other tests support the reasoning, with similar trends but reduced magnitudes.] For example, cross sections taken along a WNW–ESE line in southern Texas in the midafternoon at 2100 UTC (Fig. 12) show that the CBL deepens significantly (implied in the specific humidity field) as soil moisture decreases from the control value (Fig. 12a) to 40% less than control (Fig. 12b). Away from the front, the CBL height increases from around 1.5 km in the control run to over 2 km in the dry soil run. In the region of persistent convergence near the front, significantly more moisture is found in the layer about 2–4 km above the ground in the dry soil run than in the control run, although moisture is much less ($\sim$3–5 g kg^{-1}) nearer the ground when soil is drier. The smaller specific humidity values in the CBL are due both to reduced evaporation from the drier soil and to increased dry air entrainment effects at the top of the CBL.

Similar changes can be seen in the equivalent potential temperature (θ_E) profiles in the lower atmosphere (Fig. 13). In the control run (Fig. 13a), higher values of θ_E are present near the ground (as much as 10 K) compared to the 40% drier soil run (Fig. 13b), but more conditionally unstable conditions (larger magnitudes of $\partial\theta/\partial z$) occur above 3 km in the drier soil run. Thus, the soil moisture content influences the vertical structure of low-level stability. In the eastern portion of both cross sections, a weak capping inversion with a stable layer around 3 km was simulated.

The wind response to these CBL changes at 0000 UTC 28 May can be seen in Figs. 14 and 15. Near-surface winds (Fig. 14) are generally weaker in the KF control run (Fig. 14a) than in the run with drier soil (Fig. 14b), with much stronger thunderstorm cold pool outflow occurring near the southern Texas–Mexico border in the dry soil case. In the drier soil run, lowest model layer temperatures across much of southern Texas were 3°–4°C warmer than in the control case (not shown), with a 2°–3°C decrease in dewpoints, associated with the reduced specific humidity (Fig. 12). General southeast winds off of the Gulf of Mexico in the control run (Fig. 14a) increase by 1–3 m s^{-1} in the drier soil case (Fig. 14b). This results in a near doubling of the magnitude of simulated surface moisture convergence in the vicinity of 100°W in southern Texas during the middle and late afternoon (not shown).

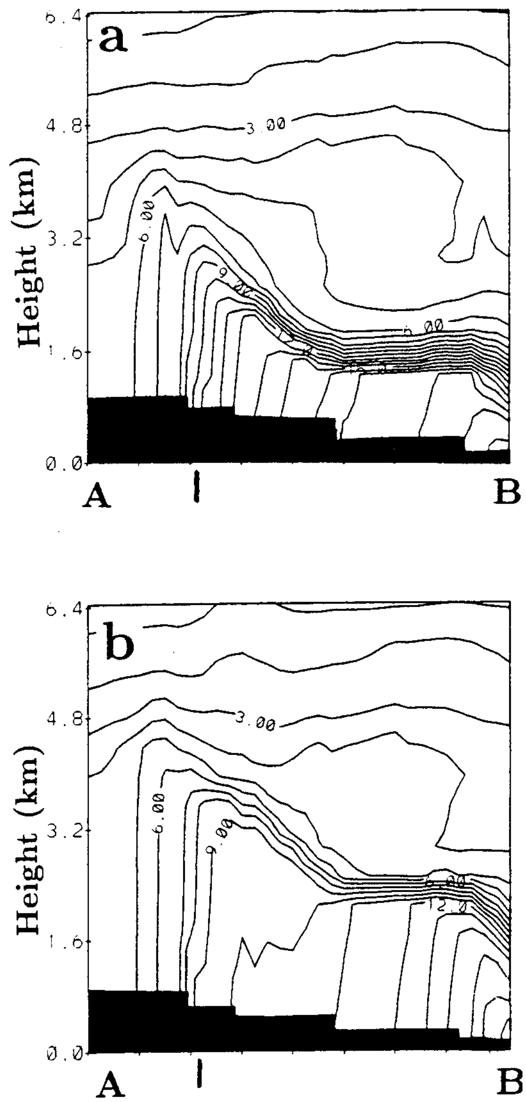

Fig. 12. Vertical cross sections of specific humidity (g kg^{-1}) taken across south Texas (shown with a line in Fig. 9) for (a) control and (b) 40% reduced soil moisture simulations with the KF scheme at 2100 UTC 27 May. Contour interval is 1 g kg^{-1}. Front location is indicated at bottom of plots.

The wind response is even greater at higher levels within the CBL (Fig. 15). Winds at $\sim$500 m above the surface are 3–5 m s^{-1} weaker in the control run (Fig. 15a) than in the drier soil run (Fig. 15b). Likewise, convergence is much stronger where the ambient southeasterly flow meets convective outflow. The increased southeasterly ambient flow should also allow for greater transport of moisture inland from the Gulf of Mexico, although in this event, the increase in moisture advection is more than offset by the reduction in moisture flux from the drier soil.

Vertical cross sections of moisture convergence (Fig.

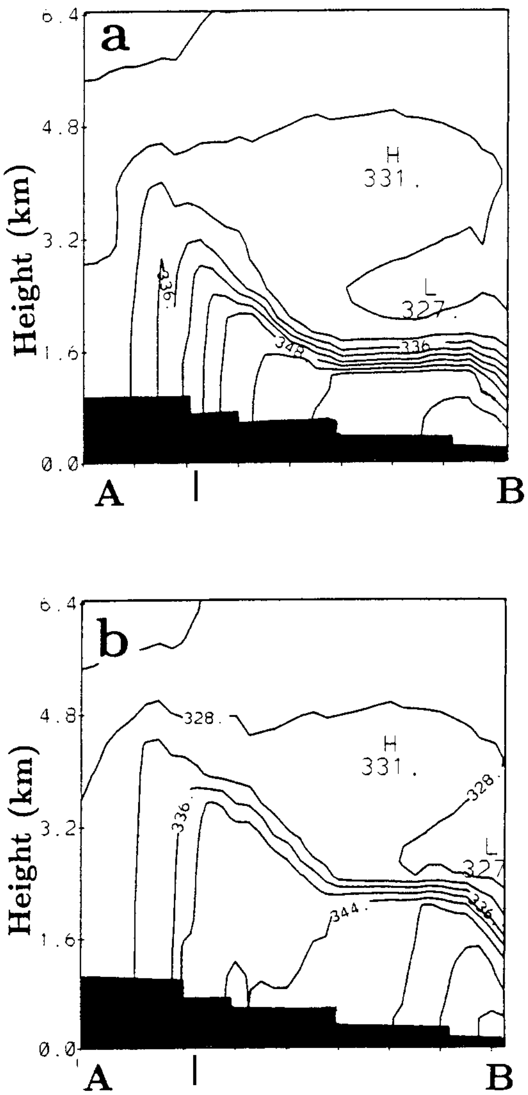

FIG. 13. As in Fig. 12 except for equivalent potential temperature (K), with contour interval of 4 K.

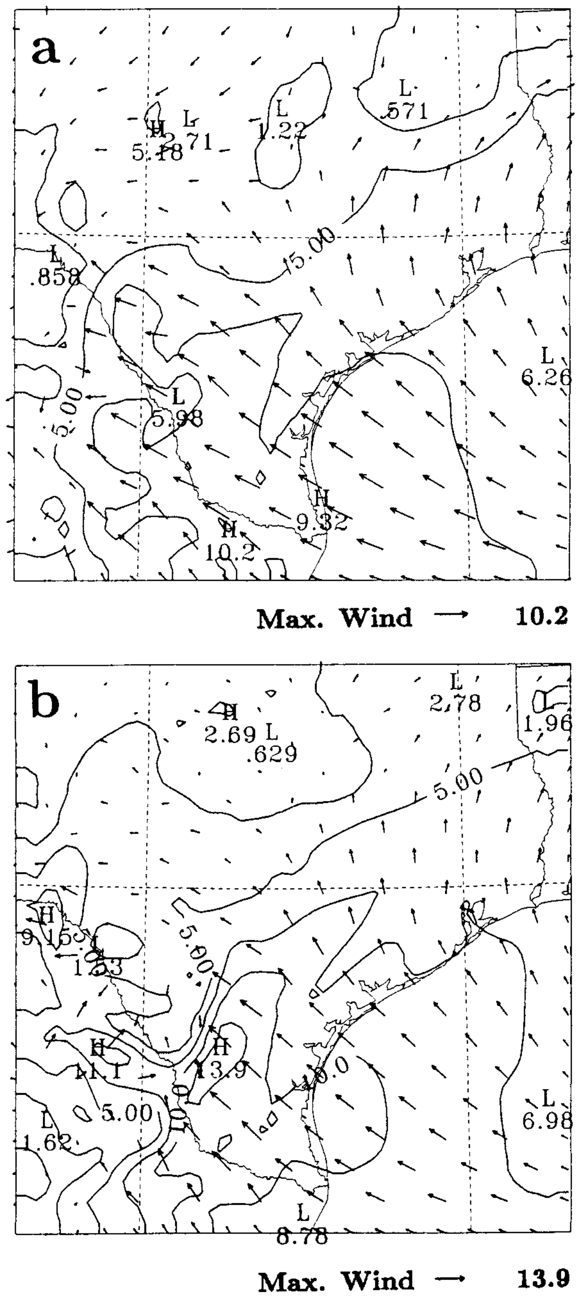

FIG. 14. Simulated lowest model layer (~70 m) winds (contours of 2.5 m s^{-1}) for (a) control and (b) 40% reduced soil moisture simulations with the KF scheme at 0000 UTC 28 May. Maximum wind speed (m s^{-1}) used for scaling of vector size is noted.

16) show that these differences in the wind field affect a fairly deep layer. In the control run (Fig. 16a) moisture convergence occurs over much of the cross section in the lowest 1000 m above the ground. Peak values of around 10×10^{-4} g kg^{-1} s^{-1} occur near the front. With the drier soil (Fig. 16b), significant moisture convergence occurs in a nearly 3000-m-deep layer farther southeast of the front compared with the control run, in a region where convective outflow impinges upon stronger ambient southeasterly flow. The peak moisture convergence is three times as large as in the control run.

Soundings in the region show that although CAPE is somewhat larger in the control run (Fig. 17a) than in the simulations with drier soil (Fig. 17b), the depth of lift required to take a parcel from its lifting condensation level to its level of free convection is reduced by over a third in the dry soil case compared with the control. This in combination with increased low-level convergence and lift would favor activation of the KF scheme in the drier soil case. In addition, winds become substantially stronger (3–4 m s^{-1}) in the drier soil case during the evening in the 800–900-mb layer (not shown), or roughly the layer where low-level jets are common in the central plains during the night. This increased strength of the low-level jet may further en-

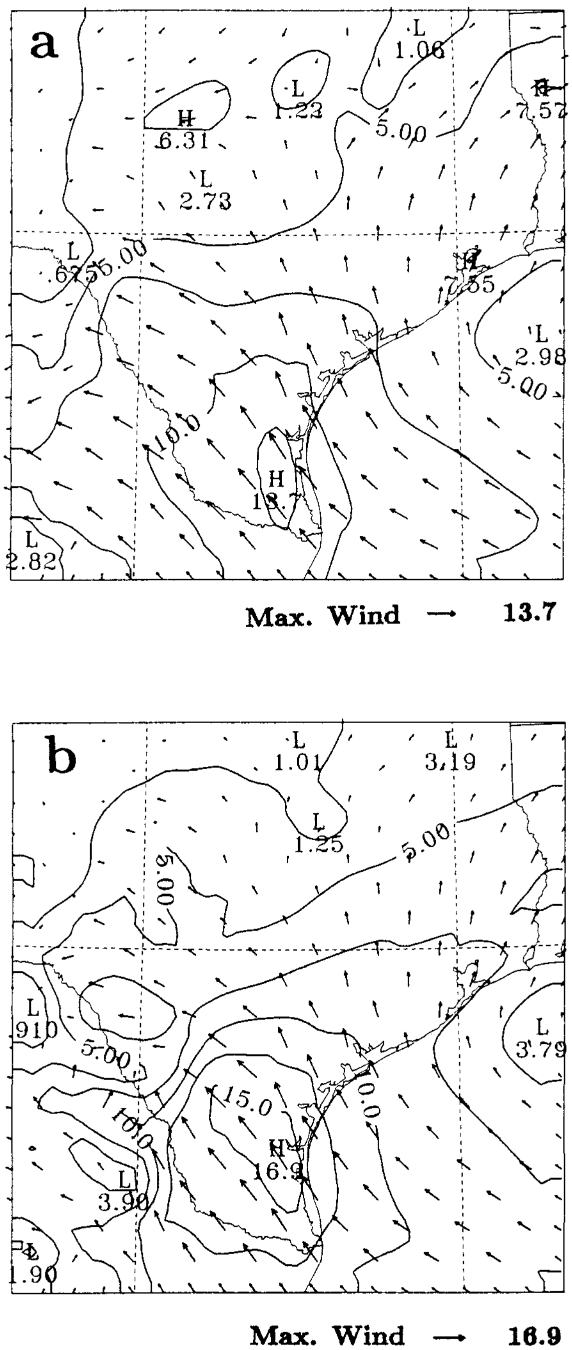

FIG. 15. As in Fig. 14 but at ~500 m above the surface.

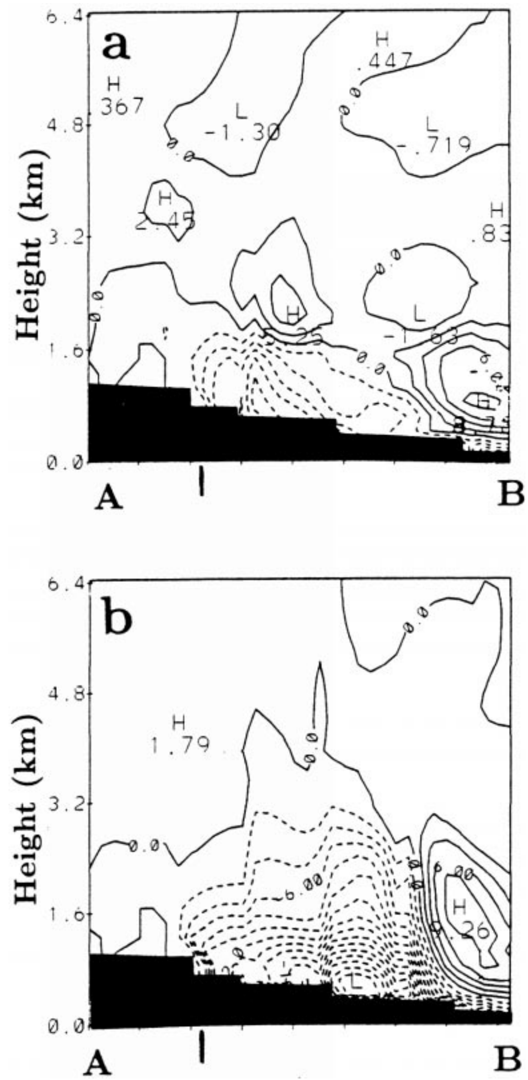

FIG. 16. As in Fig. 12 but for moisture divergence (contours every 2×10^{-4} g kg^{-1} s^{-1}) at 0000 UTC 28 May.

hance convergence at this level and act as a source of significant moisture. McCorcle (1988) also noted the influence of soil moisture on the low-level jet.

Although not shown, each of the simulations generated a region of significant rainfall north of a warm front in relatively cool, stable air over Missouri. The precipitation in this region was entirely grid resolved. Sensitivity to soil moisture in this region behaved differently from that in the highly unstable convectively active southern plains. In Missouri, the peak precipitation increased in all tests for increasing soil moisture. For both the BMJ and KF schemes, the greatest changes occurred for drier soils. Additional increases in precipitation for soils wetter than the control value were small, probably because the control volumetric soil moisture was already rather wet (33%–35%).

5) IMPACT OF SOIL MOISTURE ON CONVECTIVE PARAMETERIZATION BEHAVIOR

As shown above, the sensitivity of model QPF to soil moisture varied substantially between the convective schemes. With the BMJ scheme, results generally agreed with 1D modeling studies (e.g., Clark and Arritt 1995), showing more rainfall for wetter soil (with a few minor exceptions). Simulations with the KF scheme, however,

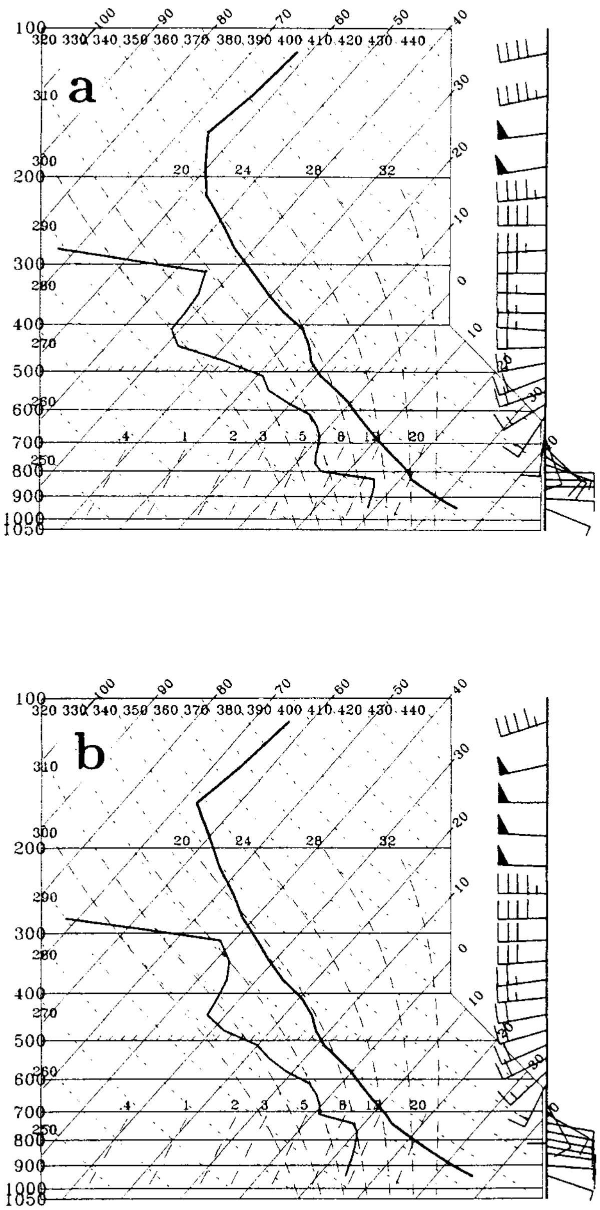

FIG. 17. Simulated soundings for a point near Cotulla, TX (COT in Fig. 2), at 2100 UTC 27 May for (a) control and (b) 40% reduced soil moisture simulations with the KF scheme.

show large increases in peak QPF with substantially drier soil.

The differing sensitivity can be explained, at least in part, by the different design of the two schemes. As described in Gallus (1999), the BMJ scheme is most likely to activate when substantial low- and midlevel moisture is present with positive CAPE. Vertical motion has no direct impact on the scheme, although it could enhance the activation of the scheme indirectly by moistening the low and middle levels of the atmosphere. Shallow convection is also taken into account in this scheme, which can redistribute heat and moisture vertically, assisting in the activation of the deep convection component. The scheme does not include a parameterized convective downdraft. These elements of the scheme, particularly the sensitivity to low- and midlevel moisture, suggest that the amount of precipitation it generates might vary directly, in a relatively straightforward fashion with soil moisture.

Unlike the BMJ scheme, the KF scheme includes parameterized moist convective downdrafts as it adjusts gridpoint temperature and moisture profiles, and it uses a trigger function based on vertical motion to determine activation. If upward motion is large enough to overcome convective inhibition, the scheme will activate. The KF scheme may be more directly influenced by surface convergence and the resulting upward motion features than the BMJ scheme, because the ascent facilitates activation. Changes in low-level thermodynamics induced by soil moisture changes will directly influence the KF scheme, possibly in a more complicated manner than the BMJ scheme. For instance, drier soil may result in reduced low-level specific humidity, but higher near-surface temperatures. The impact of the drier soil on the scheme's QPF generation may depend on the vertical temperature structure. Lower specific humidity values may result in less CAPE, but the warmer temperatures may result in less spread between the level of free convection and the lifting condensation level. Thus, in a capped situation, it may be possible for drier soil to favor KF activation, although in most cases, the scheme would likely produce less precipitation with drier soil (e.g., Clark and Arritt 1995).

In these sensitivity tests, however, it appears that ''secondary'' generation of convection accounts for the primary difference between the soil moisture–QPF sensitivity of the schemes. Because the KF scheme includes a convective downdraft, and the BMJ scheme does not, the impact of the schemes on low-level thunderstorm outflow will be distinctly different as soil moisture changes. The parameterized downdraft in the KF scheme can result in a larger decrease of low-level grid-resolved temperatures, which in turn can raise surface pressures and affect grid-resolved winds more than in simulations using the BMJ scheme. As shown earlier (Figs. 14–16), the intense rainfall in the dry soil cases with the KF scheme is related to strong moisture convergence that occurs in south Texas when thunderstorm outflow, enhanced by drier lower-tropospheric conditions, opposes increased ambient southeasterly flow from the Gulf of Mexico. In the BMJ runs, the ambient southeasterly flow present in the control run (Fig. 18a) also increases as the soil is drier (Fig. 18b). However, the lack of a parameterized convective downdraft prevents strong convective outflow from opposing the ambient flow and increasing moisture convergence in south Texas. This difference between the two schemes is of great importance in this case. It should be noted that with both schemes, the heaviest peak rainfall occurs with soil moistures intermediate between the possible

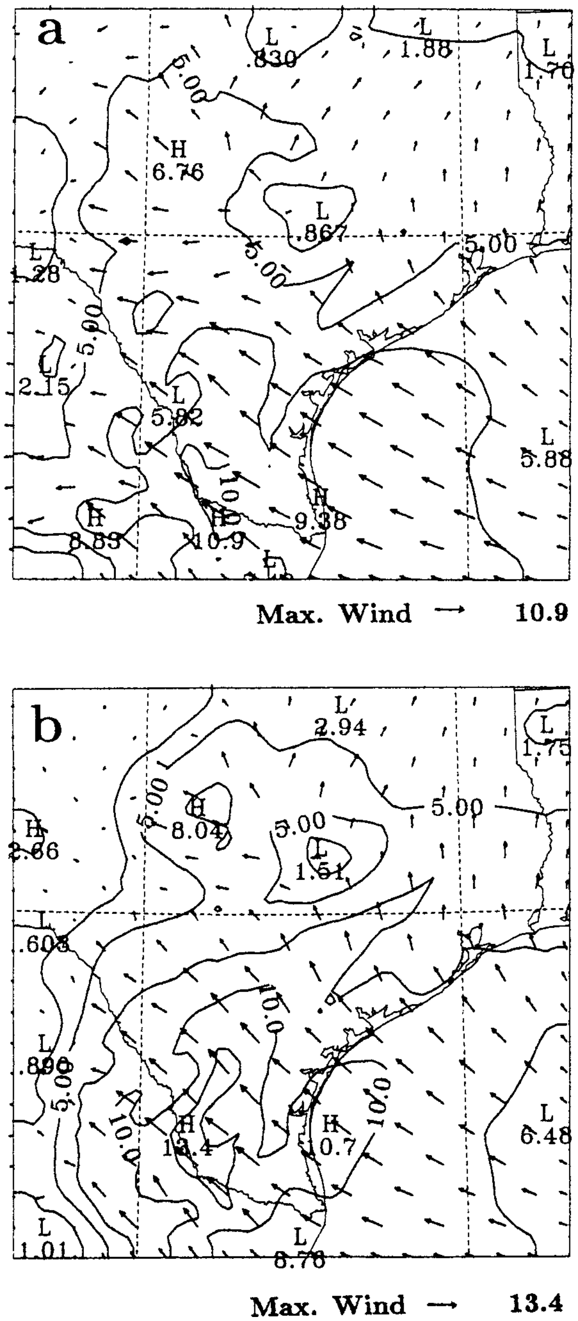

FIG. 18. As in Fig. 14 but for (a) control and (b) 40% reduced soil moisture simulations with the BMJ scheme.

range from saturation to wilting point, although the response of the schemes to quantitative changes in soil moisture is different. Tuning of the individual schemes to produce similar trends in peak precipitation may be possible.

Future work should examine other cases to determine under what conditions the subsequent generation of convection will follow the trends of this case. Forecasters using model guidance should be aware of the impact that drier soil may have on convective schemes that include parameterized convective downdrafts. During a convective event, surface observations can be examined to determine the veracity of simulated convective boundaries. Adjustments could be made to simulated QPF based on a knowledge of the convective scheme used and soil moisture data.

c. *Sensitivity to vegetation and boundary layer moisture*

1) SENSITIVITY TO VEGETATION COVERAGE

Several simulations were run to study the sensitivity of the model to vegetation coverage. Both the BMJ and KF convective parameterizations were used in simulations with the control soil moisture and in simulations with a 40% reduction in the control value of soil moisture. Higher surface latent heat fluxes were simulated in the vegetated cases.

Simulations performed with the BMJ scheme found little sensitivity of precipitation to vegetation coverage, both with the control and reduced values of soil moisture. With the KF scheme, vegetation coverage also had little impact on precipitation when the control value of soil moisture was used. However, with much drier soil (40% less), the impacts were noticeably larger (Fig. 19). Although the peak rainfall amount increased by only 12% near Cotulla in the bare soil simulation (Fig. 19b), much bigger impacts were felt throughout the precipitation region to the north where the absence of vegetation significantly lessened the rainfall, primarily during the first 12 h, in both areal coverage and amount. In general, as expected, in areas away from active precipitation, sensible heat fluxes were larger and latent heating smaller in the bare soil simulation than in the vegetated one, and this resulted in lower dewpoints and higher shelter temperatures during the afternoon. These thermodynamically less favorable conditions during the time of peak heating diminished the precipitation. Interestingly, during the following 6 h, in the evening, similar trends occurred as in the drier soil sensitivity tests. Increased low-level convergence in the bare soil case resulted in some regions of more intense rainfall than in the control case. The heavier precipitation in the region of the absolute maximum and in a small part of northeastern Texas occurred during the evening hours. The locations of some maxima (Fig. 19b) differed significantly from the run with vegetation (Fig. 19a). These results suggest that local forecast precipitation is extremely sensitive to the interaction of mesoscale and storm-induced dynamics. Under certain conditions, if the land surface modifications alter the low-level flow or the strength of thunderstorm outflows, the resulting precipitation field can differ substantially, causing significant gridpoint differences in predicted precipitation.

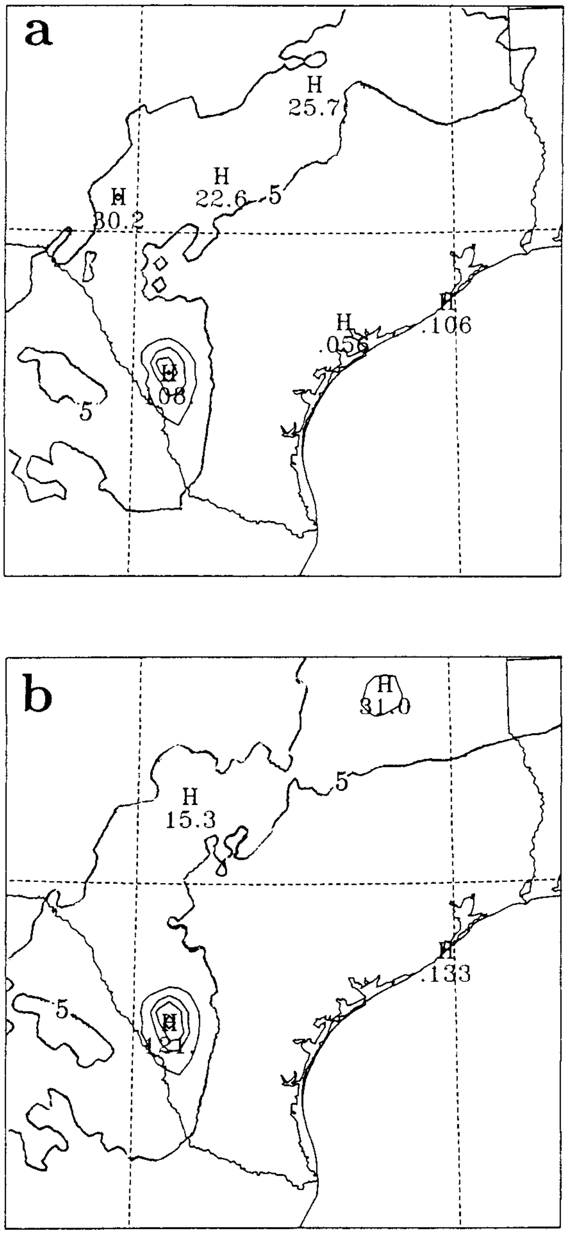

FIG. 19. Simulated precipitation (mm) for the period 1200 UTC 27 May to 0600 UTC 28 May 1997 with the KF scheme and a 40% reduction in soil moisture from the control run at 22-km horizontal resolution with (a) control vegetation and (b) no vegetation. Contouring as in Fig. 5.

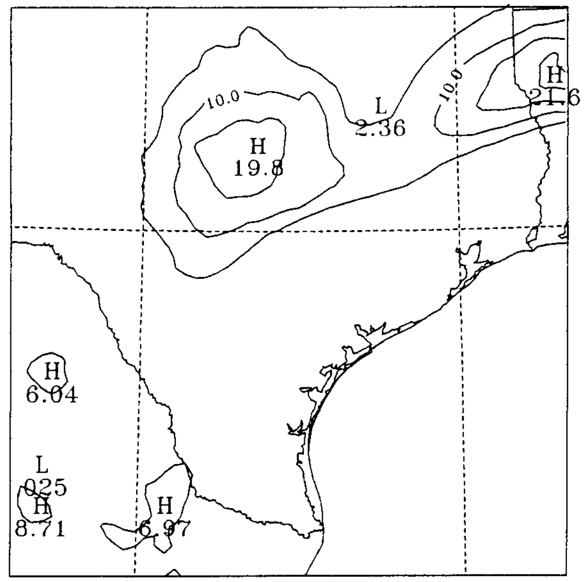

FIG. 20. Eta Model simulated precipitation (mm) for the period 1200 UTC 27 May to 0600 UTC 28 May 1997 with the BMJ scheme at 22-km horizontal resolution with coarser vertical resolution of initial data than in control run. Contour interval is 5 mm.

2) SENSITIVITY TO VERTICAL RESOLUTION OF BOUNDARY LAYER MOISTURE

An additional sensitivity test investigated the impact on simulated precipitation of the initialized boundary layer moisture field, by using coarsened vertical resolution of the initial data. This test was motivated by two issues. First, although operational models are generally able to incorporate upper air information from all significant vertical levels into their assimilation and initialization systems, many research models are initialized from datasets or model output restricted to a limited number of vertical levels, depending on the date of the event. Second, significant sensitivity to vertical distribution of low-level moisture would argue strongly for development of procedures to use nonstandard moisture data sources to improve resolution of the boundary layer moisture.

In this sensitivity test, using the BMJ scheme, accurate simulation of this event was found to depend strongly on the availability of accurate and detailed observations for the initialization of the shallow but pronounced moist layer. Because the moist layer exhibited a sharp cutoff at roughly 900 mb (Fig. 1), an initialization using only the 1000- and 850-mb level data in the lower troposphere resulted in a simulation that did not develop a convective system in south-central Texas (Fig. 20). (The control initialization used data with 50-mb vertical resolution.) Precipitation did occur in central Texas northeastward into Louisiana, with amounts similar to those in the control run (Fig. 5), but the heaviest amounts, which occurred farther south, were almost completely not simulated. The large impact of this sensitivity test has implications for both research and operational modeling. For research models, care should be taken to use output with as high a vertical resolution as is feasible. Extending the results from this test also implies that data assimilation systems should seek to use as much information on the lower-tropospheric moisture structure as possible, with careful attention to accuracy of the data.

Other studies have indicated that the operational Eta Model underestimated the degree of thermodynamic instability during this event (D. Gray, NESDIS, 1998, personal communication). The high-resolution runs in this study imply that accurate depiction of the strong moisture convergence was necessary to maintain extreme instability in the face of daytime sensible heating, which increased the boundary layer depth, mixing the much drier air around 850 mb downward. Accurate depiction of the low-level moisture profile was essential so that precipitation could occur later in south Texas in the model. The model sensitivity to the representation of lower-tropospheric moisture exceeded that of even the most extreme soil moisture variations. This result argues strongly for accurate assimilation of all information helping to define the boundary layer moisture field, especially for cases such as this one where an elevated mixed layer with greatly diminished moisture overlies the lower moist layer.

6. Conclusions

A series of sensitivity tests were performed using a 22-km horizontal resolution version of the NCEP Eta Model to investigate the impact of soil moisture on forecasts of a Texas convective system. The convection in this event occurred in an environment that was originally strongly capped with only a shallow moist boundary layer present. Significant evapotranspiration and strong moisture convergence along a nearly stationary front across central Texas, accompanied by additional lift from a southwestward-propagating gravity wave, conditioned the atmosphere for the convection that would develop later. Convective initiation occurred in a region where conditional static instability became extreme. The convective system propagated south-southwestward, a motion strongly deviant to the mean flow.

Although the volumetric soil moisture field for this event lacked strong gradients across Texas and presumably did not play a significant role in the evolution of convection (i.e., through inducing thermal circulations), the important role that mesoscale features played in the event suggests that this is a good case to use in an investigation of the potential impacts of soil moisture on convective evolution. Sensitivity tests using this event indicate that domain total precipitation generally varies directly with soil moisture, although behavior is dependent upon the convective scheme used. Similar conclusions have been reached by Pan et al. (1996), though with a different model and convective schemes, as well as in a different geographical location with different precipitation systems. The general trend for increasing precipitation with increased soil moisture due to improved thermodynamic conditions agrees with other studies (e.g., Clark and Arritt 1995) that have found increases in soil moisture in nonfrontal situations and the ensuing increases in latent heat fluxes to be thermodynamically conducive to increased precipitation over what would occur with drier soil. However, peak rainfall in the region of most intense model convection in this event exhibited a much different behavior.

As initial soil moisture is increased, peak precipitation increases to a point, but further increases in soil moisture then reduce the peak rainfall. With the KF scheme, whose trigger function is directly related to vertical motion, wetter soil generally results in less peak precipitation than drier soil in the Texas region. With the BMJ scheme, which responds strongly to low- and midlevel moisture, wetter soils result in greater peak precipitation, although the maximum does not occur with the wettest soil.

When soil moisture is decreased, the evening convective system that occurs to the south of the afternoon convection generally becomes more intense. With the BMJ scheme, this was true only for a limited range of decreased soil moisture from the control value. With the KF scheme, drier soil greatly increased peak precipitation. Enhanced low-level convergence influenced by the increased sensible heat flux and strengthened thunderstorm outflow in the KF runs is suggested to result in more intense model storms during the evening hours in this case.

These results suggest that the dynamic consequences (e.g., modifications in wind fields) of changes in soil moisture may dominate over the thermodynamic changes in affecting precipitation in some regions within a short-range forecast, even when soil moisture gradients are weak. Although increased soil moisture and larger latent heat fluxes generally increase lower-tropospheric moisture, the reduced sensible heat fluxes alter the strength of existing low-level circulations and convergence. Decreased soil moisture is associated with changes in CBL turbulence and consequently modification of the flow. It may result in enhanced convergence that is able to produce more intense precipitation systems with far greater peak rainfalls despite a general tendency for the lower troposphere to be drier.

The simulation of such processes in numerical models is strongly dependent on the behavior of the convective parameterization. Knowledge that the KF scheme includes a parameterized convective downdraft, unlike the BMJ scheme, could assist forecasters in interpreting model guidance. Models using parameterizations such as KF may be expected to show greater QPF–soil moisture sensitivity when soil is dry, due to the increased intensity of convectively induced low-level flows, and enhanced potential for interaction of these flows with ambient winds or other mesoscale circulations. Forecasters should closely monitor surface observations in these cases to determine the veracity of simulated convective outflows, and use this information to adjust QPF. In addition, forecasters should be aware of general soil moisture conditions in their regions, and efforts should be made to provide them with additional soil moisture data that could be compared with model-initialized fields.

Acknowledgments. The authors would like to thank Drs. Eric Rogers and Tom Black, and Mike Baldwin at NCEP for providing a few fields necessary for running the model. Additional thanks are given to Dr. John Kain for assistance in implementing the Kain–Fritsch scheme, and to three anonymous reviewers for suggestions that improved the paper. This work was sponsored by National Science Foundation/National Oceanic and Atmospheric Administration Grants ATM-9612388 and ATM-9908932 in the USWRP program. This is Journal Paper J-18483 of the Iowa Agricultural and Home Economics Experiment Station, Ames, Iowa, Projects 3435 and 3245, supported by the Hatch Act and the State of Iowa.

REFERENCES

Becker, A., H. Kraus, and C. M. Ewenez, 1997: On the variety of cold fronts: Two-dimensional numerical simulations. *Beitr. Phys. Atmos.,* **70,** 265–283.

Betts, A. K., 1986: A new convective adjustment scheme. Part I: Observational and theoretical basis. *Quart. J. Roy. Meteor. Soc.,* **112,** 677–692.

——, and M. J. Miller, 1986: A new convective adjustment scheme. Part II: Single column tests using GATE wave, BOMEX, and arctic air-mass data sets. *Quart. J. Roy. Meteor. Soc.,* **112,** 693–709.

Bluestein, H. B., 1993: *Synoptic-Dynamic Meteorology in Midlatitudes.* Volume II. Oxford University Press, 594 pp.

Chang, J.-T., and P. J. Wetzel, 1991: Effects of spatial variations of soil moisture and vegetation on the evolution of a prestorm environment: A numerical case study. *Mon. Wea. Rev.,* **119,** 1368–1390.

Chen, F., and Coauthors, 1996: Modeling of land surface evaporation by four schemes and comparison with FIFE observations. *J. Geophys. Res.,* **101,** 7251–7277.

Clapp, R. B., and G. M. Hornberger, 1978: Empirical equations for some soil hydraulic properties. *Water Resour. Res.,* **14,** 601–604.

Clark, C. A., and R. W. Arritt, 1995: Numerical simulations of the effect of soil moisture and vegetation cover on the development of deep convection. *J. Appl. Meteor.,* **34,** 2029–2045.

Corfidi, S. F., 1998: Some thoughts on the role of mesoscale features played in the 27 May 1997 central Texas tornado outbreak. Preprints, *19th Conf. on Severe Local Storms,* Minneapolis, MN, Amer. Meteor. Soc., 177–180.

Cosby, B. J., G. M. Hornberger, R. B. Clapp, and T. R. Ginn, 1984: A statistical exploration of the relationships of soil moisture characteristics to the physical properties of soil. *Water Resour. Res.,* **20,** 682–690.

Darkow, G. L., and D. W. McCann, 1977: Relative environmental winds for 121 tornado bearing storms. Preprints, *11th Conf. on Severe Local Storms,* Omaha, NE, Amer. Meteor. Soc., 413–417.

Gallus, W. A., Jr., 1999: Eta simulations of three extreme precipitation events: Impact of resolution and choice of convective parameterization. *Wea. Forecasting,* **14,** 405–426.

——, and M. Segal, 1999: Diabatic effects on late winter cold front evolution: Conceptual and numerical model evaluations. *Mon. Wea. Rev.,* **127,** 1518–1537.

Gerrity, J. P., T. L. Black, and R. E. Treadon, 1994: On the numerical solution of the Mellor–Yamada level 2.5 turbulent kinetic energy equation in the Eta Model. *Mon. Wea. Rev.,* **122,** 1640–1646.

Holtslag, A. A., and M. Ek, 1996: Simulation of surface fluxes and boundary layer development over the pine forest in HAPEX-MOBILHY. *J. Appl. Meteor.,* **35,** 202–213.

Janjic, Z. I., 1994: The step-mountain eta coordinate model: Further developments of the convection, viscous sublayer and turbulence closure schemes. *Mon. Wea. Rev.,* **122,** 928–945.

Kain, J. S., and J. M. Fritsch, 1993: Convective parameterization for mesoscale models: The Kain–Fritsch scheme. *The Representation of Cumulus Convection in Numerical Models, Meteor. Monogr.,* No. 46, Amer. Meteor. Soc., 165–170.

Koch, S. E., A. Aksakal, and J. T. McQueen, 1997: The influence of mesoscale humidity and evapotranspiration field in model forecast of cold-frontal squall line. *Mon. Wea. Rev.,* **125,** 384–409.

Lanicci, J. M., T. N. Carlson, and T. T. Warner, 1987: Sensitivity of the Great Plains severe storm environment to soil moisture distribution. *Mon. Wea. Rev.,* **115,** 2660–2673.

Lobocki, L., 1993: A procedure for the derivation of surface-layer bulk relationships from simplified second-order closure models. *J. Appl. Meteor.,* **32,** 126–138.

McCorcle, M. D., 1988: Simulation of surface-moisture effects on the Great Plains low-level jet. *Mon. Wea. Rev.,* **116,** 1705–1720.

Mellor, G. L., and T. Yamada, 1974: A hierarchy of turbulence closure models for planetary boundary layers. *J. Atmos. Sci.,* **31,** 1791–1806.

——, and ——, 1982: Development of a turbulence closure model for geophysical fluid problems. *Rev. Geophys. Space Phys.,* **20,** 851–875.

Mesinger, F., Z. I. Janjic, S. Nickovic, D. Gavrilov, and D. G. Deaven, 1988: The step mountain coordinate: Model description and performance for cases of Alpine cyclogenesis and for a case of an Appalachian redevelopment. *Mon. Wea. Rev.,* **116,** 1493–1518.

Noilhan, J., and S. Planton, 1989: A simple parameterization of land surface processes for meteorological models. *Mon. Wea. Rev.,* **117,** 536–549.

Ookouchi, Y., M. Segal, R. C. Kessler, and R. A. Piekle, 1984: Evaluation of soil moisture effects on generation and modification of mesoscale circulations. *Mon. Wea. Rev.,* **112,** 2281–2292.

Pan, H.-L., and L. Mahrt, 1987: Interaction between soil hydrology and boundary-layer development. *Bound.-Layer Meteor.,* **38,** 185–202.

Pan, Z., E. S. Takle, M. Segal, and R. W. Turner, 1996: Influence of model parameterization schemes on the response of rainfall to soil moisture in the central United States. *Mon. Wea. Rev.,* **124,** 1786–1802.

Rasmussen, E. N., and R. B. Wilhelmson, 1983: Relationships between storm characteristics and 1200 GMT hodographs, low-level shear, and stability. Preprints, *13th Conf. on Severe Local Storms,* Tulsa, OK, Amer. Meteor. Soc., J5–J8.

Segal, M., W. L. Physick, J. Heim, and R. W. Arritt, 1993: On the enhancement of cold front temperature contrasts by differential cloud cover. *Mon. Wea. Rev.,* **121,** 867–873.

——, R. W. Arritt, C. Clark, R. Rabin, and J. Brown, 1995: Scaling evaluation of the effect of surface characteristics on potential for deep convection over uniform terrain. *Mon. Wea. Rev.,* **123,** 383–400.

Warner, T. T., R. A. Peterson, and R. E. Treadon, 1997: A tutorial on lateral boundary conditions as a basic and potentially serious limitation to numerical weather prediction. *Bull. Amer. Meteor. Soc.,* **78,** 2599–2617.

Yucel, I., W. J. Shuttleworth, J. Washburne, and F. Chen, 1998: Evaluating NCEP Eta Model–derived data against observations. *Mon. Wea. Rev.,* **126,** 1977–1991.

Zhao, Q., F. H. Carr, and G. B. Lesins, 1991: Improvement of precipitation forecasts by including cloud water in NMC's Eta Model. Preprints, *Ninth Conf. on Numerical Weather Prediction,* Denver, CO, Amer. Meteor. Soc., 50–53.

Zobler, L., 1986: A world soil file for global climate modeling. NASA TM-87802, National Aeronautics and Space Administration, 32 pp. [Available from GISS, 2880 Broadway, New York, NY 10025.]